Pulse breaking recovery in fiber lasers

L. M. Zhao[1,2], D. Y. Tang[1]*, H. Y. Tam[3], and C. Lu[2]

[1] *School of Electrical and Electronic Engineering, Nanyang Technological University, Singapore 639798*
[2] *Department of Electronic and Information Engineering, Hong Kong Polytechnic University, Hung Hom, Hong Kong, China*
[3] *Department of Electrical Engineering, Hong Kong Polytechnic University, Hung Hom, Hong Kong, China*
[*] *Corresponding author: edytang@ntu.edu.sg*

Abstract: Pulse breaking recovery is numerically demonstrated in dispersion-managed fiber lasers designed for generating high peak power ultrashort optical pulses. It is shown that due to the cavity boundary condition, local pulse breaking can be absorbed by the pulse propagation in erbium-doped fiber with normal dispersion. Consequently, high peak power transform-limited pulses beyond the gain-bandwidth limitation could be generated.

OCIS codes: (060.5530) Pulse propagation and temporal solitons; (140.3510) Lasers, fiber; (190.5530) Pulse propagation and temporal solitons.

References and links

1. K. Tamura, E. P. Ippen, H. A. Haus, and L. E. Nelson, "77-fs pulse generation from a stretched-pulse mode-locked all-fiber ring laser," Opt. Lett. **18**, 1080-1082 (1993).
2. F. Ö. Ilday, J. R. Buckley, W. G. Clark, and F. W. Wise, "Self-similar evolution of parabolic pulses in a laser," Phys. Rev. Lett. **92**, 213902 (2004).
3. L. M. Zhao, D. Y. Tang, T. H. Cheng, and C. Lu, "Ultrashort pulse generation in lasers by nonlinear pulse amplification and compression," Appl. Phys. Lett. **90**, 051102 (2007).
4. M. E. Fermann, V. I. Kruglov, B. C. Thomsen, J. M. Dudley, and J. D. Harvey, "Self-Similar Propagation and Amplification of Parabolic Pulses in Optical Fibers," Phys. Rev. Lett. **84**, 6010-6013 (2000).
5. W. J. Tomlinson, R. H. Stolen, and A. M. Johnson, "Optical wave breaking of pulses in nonlinear optical fibers," Opt. Lett. **10**, 457-459 (1985).
6. D. Anderson, M. Desaix, M. Lisak, and M. L. Quiroga-Teixeiro, "Wave breaking in nonlinear-optical fibers," J. Opt. Soc. Am. B **9**, 1358-1361 (1992).
7. L. F. Mollenauer, R. H. Stolen, J. P. Gordon, and W. J. Tomlinson, "Extreme picosecond pulse narrowing by means of soliton effect in single-mode optical fibers," Opt. Lett. **8**, 289-291 (1983).
8. J. C. Bronski and J. N. Kutz, "Numerical simulation of the semi-classical limit of the focusing nonlinear Schrödinger equation," Phys. Lett. **254**, 325-336 (1999).
9. D. Krylov, L. Leng, K. Bergman, J. C. Bronski, and J. N. Kutz, "Observation of the breakup of a prechirped N-soliton in an optical fiber," Opt. Lett. **24**, 1191-1193 (1999).
10. D. Y. Tang, L. M. Zhao, B. Zhao, A. Q. Liu, "Mechanism of multisoliton formation and soliton energy quantization in passively mode-locked fiber lasers," Phys. Rev. A **72**, 043816 (2005).
11. L. M. Zhao, D. Y. Tang, J. Wu, X. Q. Fu, and S. C. Wen, "Noise-like pulse in a gain-guided soliton fiber laser," Opt. Express, **15**, 2145-2150 (2007).

1. Introduction

Recently, study on the high power ultrashort pulse fiber lasers attracted considerable attention [1-3]. The conventional mode-locked fiber lasers make use of the optical soliton feature for the ultrashort pulse generation. Although ultrashort pulses with sub-picosecond duration could be routinely generated, due to the strong nonlinearity of the laser cavity, energy of the formed soliton pulse was limited in the tens of pico-joule level. To overcome the limitation caused by the large cavity nonlinearity, Tamura et al. proposed a technique of the so-called stretched pulse operation of mode-locked fiber lasers [1]. The main idea of the technique is using fibers of opposite dispersion to construct the laser cavity. When a pulse circulates in the cavity, its pulse width is periodically stretched and compressed. On average the pulse peak power is reduced compared with that of the equivalent soliton operation of the laser. Therefore, pulses with larger energy could be obtained. Based on the parabolic pulse formation in positive dispersion gain media [4], Ilday et al. further proposed a technique for achieving the self-

#95964 - $15.00 USD Received 8 May 2008; revised 25 Jun 2008; accepted 13 Jul 2008; published 28 Jul 2008

similar pulse operation of the mode-locked fiber lasers [2]. With the technique they have demonstrated large energy mode locked pulses. However, neither of the above techniques could generate ultrashort pulses directly from the laser oscillator. We have also proposed a technique for the generation of high peak power ultrashort pulses directly from a fiber laser oscillator [3]. It was shown that by taking advantage of the nonlinear pulse amplification in a positive dispersion fiber and subsequently nonlinearly compressing the pulse in a negative dispersion fiber within a laser cavity, high peak power transform-limited ultrashort pulses with spectral width beyond the laser gain bandwidth could be generated.

It is well-known that propagation of an intense optical pulse in positive dispersion fibers could cause wave breaking [5, 6]. Moreover, propagation of an intense pulse in a negative dispersion fiber results in soliton shaping of the pulse and formation of pulse pedestal [7]. Pulse breaking caused by the propagation of a prechirped intense pulse in an anomalous dispersive fiber has been demonstrated numerically [8] and experimentally [9]. As with our technique [3] the nonlinear pulse compression in the anomalous dispersive fiber is used to generate ultrashort pulse, it would be expected that satellite pulses or pulse breaking could be generated during the nonlinear pulse compression process. In the case of strong laser gain, these broken pulses could be further amplified and lead to the formation of multiple-pulse laser operation. Indeed, in the practice if the laser parameters are not appropriately selected, multiple pulse operation of the fiber lasers has been observed. However, we show in this paper numerically that with careful control of the laser parameters and operation condition, satellite pulse generation or pulse breaking caused by the aforementioned nonlinear compression process could be absorbed by the pulse propagation in the cavity. As a consequence of the pulse breaking recovery high peak power transform-limited pulses are generated in the lasers.

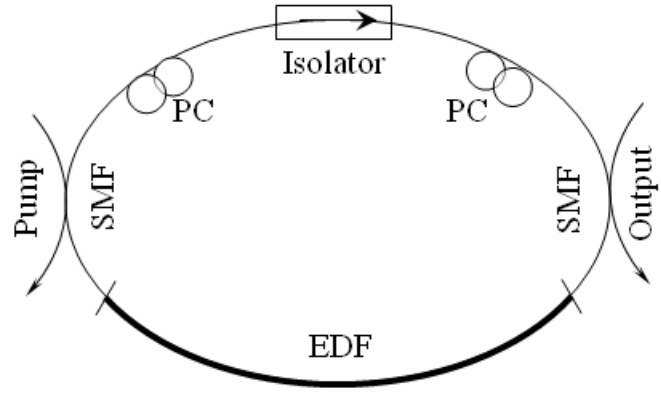

Fig. 1. Schematic of the fiber laser. PC: polarization controller; SMF: single-mode fiber; EDF: erbium-doped fiber.

2. Laser schematic and numerical results

To implement the nonlinear pulse amplification and compression techniques in one round trip of a laser cavity, a dispersion-managed fiber cavity is required. Therefore, we used a fiber laser as schematically shown in Fig. 1 to illustrate the pulse breaking recovery effect in the lasers. The cavity is a unidirectional ring comprising a segment of erbium-doped fiber (EDF) with normal group velocity dispersion, and two segments of standard single mode fibers (SMFs) separated by a polarization dependent isolator (PDI). The PDI is required for the self-started laser mode-locking as the nonlinear polarization rotation (NPR) mode locking technique is used. A 10% fiber coupler is used as the laser output.

To faithfully simulate the pulse evolution in the laser cavity, we used the round-trip model as described in [10] for our simulations. Briefly, the light propagation in the fibers is described by the coupled Ginzburg-Landau equations:

#95964 - $15.00 USD Received 8 May 2008; revised 25 Jun 2008; accepted 13 Jul 2008; published 28 Jul 2008

$$\begin{cases} \dfrac{\partial u}{\partial z} = -i\beta u + \delta \dfrac{\partial u}{\partial t} - \dfrac{ik''}{2}\dfrac{\partial^2 u}{\partial t^2} + \dfrac{ik'''}{6}\dfrac{\partial^3 u}{\partial t^3} + i\gamma(|u|^2 + \dfrac{2}{3}|v|^2)u + \dfrac{i\gamma}{3}v^2u^* + \dfrac{g}{2}u + \dfrac{g}{2\Omega_g^2}\dfrac{\partial^2 u}{\partial t^2} \\ \dfrac{\partial v}{\partial z} = i\beta v - \delta \dfrac{\partial v}{\partial t} - \dfrac{ik''}{2}\dfrac{\partial^2 v}{\partial t^2} + \dfrac{ik'''}{6}\dfrac{\partial^3 v}{\partial t^3} + i\gamma(|v|^2 + \dfrac{2}{3}|u|^2)v + \dfrac{i\gamma}{3}u^2v^* + \dfrac{g}{2}v + \dfrac{g}{2\Omega_g^2}\dfrac{\partial^2 v}{\partial t^2} \end{cases} \quad (1)$$

where u and v are the normalized envelopes of the optical pulses along the two orthogonal polarization axes of the fiber, u^* and v^* are the conjugate of u and v. $2\beta = 2\pi\Delta n/\lambda$ is the wave-number difference between the two polarization modes of the fiber, where Δn is the difference between the effective indices of the two modes, λ is the wavelength. $2\delta = 2\beta\lambda/2\pi c$ is the inverse group velocity difference, where c is the light speed. k'' is the second order dispersion coefficient, k''' is the third order dispersion coefficient and γ represents the nonlinearity of the fiber. g is the saturable gain of the fiber and Ω_g is the bandwidth of the laser gain. For undoped fibers $g = 0$, for the erbium-doped fiber, we further considered the gain saturation as:

$$g = G\exp[-\frac{\int(|u|^2 + |v|^2)dt}{P_{sat}}] \quad (2)$$

where G is the small signal gain coefficient and P_{sat} is the normalized saturation energy.

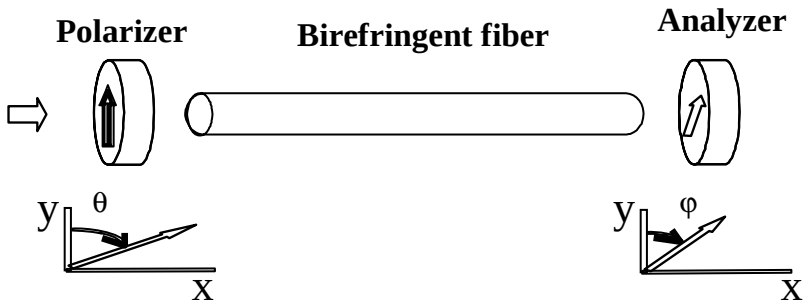

Fig. 2. Mathematically simplified laser cavity.

The light transmission through the setup can be calculated by using the Jones matrix method. The cavity of the fiber laser is equivalently simplified as shown in Fig. 2. Assuming that the two principal polarization axes of the birefingent fiber are the x (horizontal) and y (vertical) axis; the polarizer and the analyzer are set in such positions that their polarization directions have an angle of θ and φ to the y axis of the fiber polarization, respectively. Then the intensity transmission T of light through the setup is:

$$T = \sin^2\theta\sin^2\varphi + \cos^2\theta\cos^2\varphi + \frac{1}{2}\sin 2\theta\sin 2\varphi\cos[\Phi_l + \Phi_{nl}] \quad (3)$$

where Φ_l is the linear phase delay and Φ_{nl} is the nonlinear phase delay.

Numerically we found that once the orientations of the polarizer and analyzer with respect to the fiber polarization principal axes are fixed, the linear transmission of the setup is a sinusoidal function of the linear phase delay between the two polarization components.

#95964 - $15.00 USD Received 8 May 2008; revised 25 Jun 2008; accepted 13 Jul 2008; published 28 Jul 2008

The orientation of the polarizer determines the projection of light on the two polarization axes of the fiber, therefore, determines whether positive Φ_{nl} or negative Φ_{nl} would be generated. Assuming that negative Φ_{nl} is generated, then further depending on the linear phase delay, the NPR could cause either an increase or decrease in the intensity transmission. The magnitude of Φ_{nl} is always proportional to the intensity of light. This means that with the increase of the light intensity, either an increase or a decrease in the transmission could be generated, which is purely determined by the linear phase delay selection.

In the practice it is difficult to set the linear phase delay just within the range where the saturable absorption effect is achieved. Therefore, one or two sets of polarization controller (PC) is normally inserted in the setup, as shown in Fig. 1, to efficiently control the value of the linear phase delay. Mathematically, this is equivalent to add a variable linear phase delay bias term in the intensity transmission formula. Hence the intensity transmission can be further written as:

$$T = \sin^2\theta\sin^2\varphi + \cos^2\theta\cos^2\varphi + \frac{1}{2}\sin 2\theta \sin 2\varphi \cos\left[\Phi_{PC} + \Phi_{Fiber}\right] \tag{4}$$

where Φ_{PC} is the phase delay bias introduced by the PC and it is continuously tunable, Φ_{Fiber} is the phase delay resulted from the fiber including both the linear phase delay and the nonlinear phase delay. With the help of the PC, it is always possible to achieve an artificial saturable absorber effect through changing the linear birefringence in the cavity.

We start the simulation with an arbitrary weak pulse and let it circulate in the laser cavity. Whenever the pulse encounters an individual intracavity component, we multiply the Jones matrix of the component to the pulse field to account the effect of the cavity component. The calculation is continued until a steady pulse evolution state is established. The parameters shown in Table 1 were used for our simulations. The laser cavity length $L=1_{SMF}+3_{EDF}+1_{SMF}+10\%Output+1_{SMF}=6$ m. An insertion loss of 3 dB for the mode-locking section (PC-Isolator-PC) was also considered.

Table 1. Parameters used in the simulations

γ	3 $W^{-1}km^{-1}$	k''_{EDF}	40.8 ps^2/km
k''_{SMF}	-22.9 ps^2/km	k'''	-0.127 ps^3/km
L/L_b	2	Ω_g	16 nm
θ	0.152π	φ	$\theta+\pi/2$
P_{sat}	1 nJ	G	varying
Φ_{PC}	varying between π to 2π (mode locking regime)		

Figure 3 shows the simulation results obtained when the cavity linear phase delay bias is set at $\Phi_{PC}=1.7\pi$ and the laser gain is varied. Because the net cavity dispersion is large normal, the gain-guided solitons (GGSs) are formed in the laser. The optical spectra of the solitons are characterized by their steep spectral edges. The stronger the pump power, the narrower the soliton pulse width, and the broader the soliton spectral bandwidth. As the increment of the soliton spectral bandwidth is far larger than the decrement of the soliton pulse width, numerical calculations show that the generated GGSs are strongly chirped, and the stronger the pump power, the larger time-bandwidth-product (TBP) i.e. larger pulse chirp is. The calculated TBP is 5.34, 6.02, and 6.31, respectively, for G=1100, G=1200, and G=1300.

#95964 - $15.00 USD Received 8 May 2008; revised 25 Jun 2008; accepted 13 Jul 2008; published 28 Jul 2008

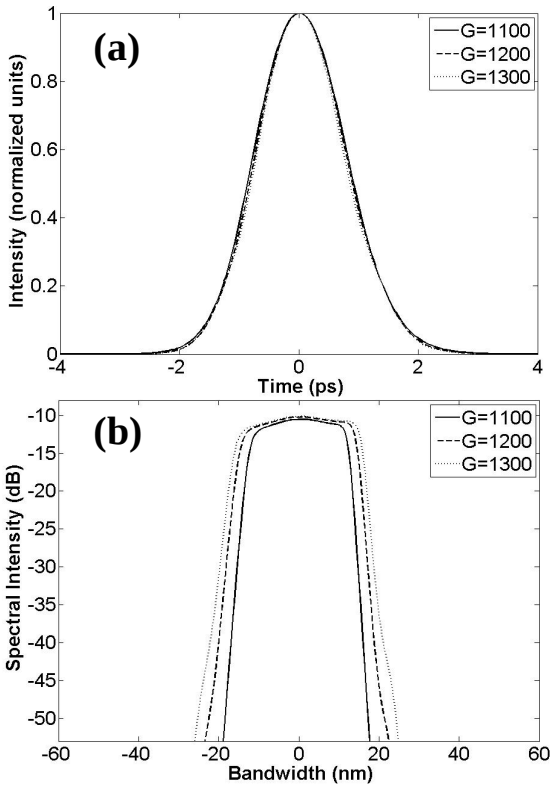

Fig. 3. Simulation results of gain-guided solitons under different pump strength at Φ_{PC} =1.7π. (a) autocorrelation trace, (b) optical spectrum.

The detailed soliton evolution in the cavity was numerically studied. Propagating in the normal dispersion gain fiber, the pulse is amplified and strongly chirped. The pulse then propagates in the SMF with anomalous dispersion, where it is de-chirped and compressed. Figure 4(a) shows a case of the pulse evolution with Φ_{PC} =1.7π and G=1300. In this case the pulse energy after amplification is not strong. Video A shows the detailed pulse chirp accumulation (pulse amplification) and de-chirped process in SMFs (the length step is 0.1m) corresponding to Fig. 4(a). Figure 4(b) shows another case of stable pulse propagation in cavity with Φ_{PC} =1.85π and G=1400. As the amplified pulse now has large pulse energy, nonlinear pulse compression becomes significant as the pulse propagates in the SMFs. As shown in video B, due to the strong local nonlinearity, pulse breaking occurs in the SMFs Consequently two broken pulses with low peak power are generated. However, as the pulse subsequently propagates in the EDF, the pulse breaking is stopped, and eventually a single pulse is recovered. The result shows that even under existence of the local pulse breaking the laser can still emit stable single mode-locked pulse. We note that the pulse shaping caused by the mode-locking effect of the laser (or passing through the mode-locking section) and the 3-dB insertion loss is reflected by the pulse difference between the starting and ending points shown in Fig. 4.

Further increasing the pump strength, although the details of the pulse breaking vary, within a certain pump strength range the similar local pulse breaking and recovering feature remain. With too strong pump power the laser will emit noise-like pulses [12]. Numerical simulations suggested that the pulse breaking recovery is a general feature of the fiber laser. And it is because of the feature the laser can generate stable high peak power ultra narrow pulses directly from the cavity. As pulse breaking in the laser is always associated with the

#95964 - $15.00 USD Received 8 May 2008; revised 25 Jun 2008; accepted 13 Jul 2008; published 28 Jul 2008

strong nonlinear pulse compression and shaping, the self-phase modulation, cross-phase modulation, and four-wave mixing between the two orthogonal polarization components of the pulse causes significant pulse spectral broadening, consequently, transform-limited pulse with bandwidth beyond the gain-bandwidth limitation could be generated. Obviously, depending on the pump strength there are three operation regimes of the fiber lasers before the appearance of multiple-pulse operation: the GGS operation, the high peak power ultra narrow pulse operation, and the noise-like pulse operation. Our numerical simulation turned out that apart from the pulse peak clamping that could cause noise-like pulse emission in the laser, the strong nonlinear pulse shaping in the cavity could also lead to noise-like pulse emission. In addition, our numerical simulations have shown that the parameter regimes of the three types of laser operation are strongly related to the laser output position and the output coupling strength.

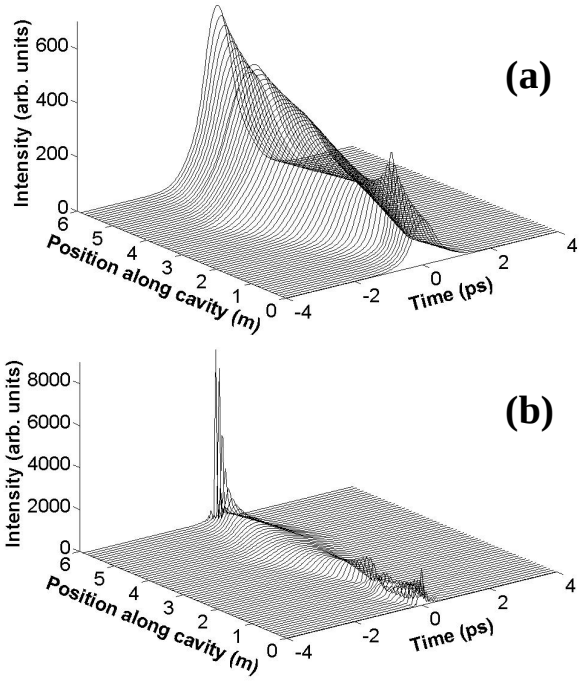

Fig. 4. Numerically calculated pulse evolution in cavity. (a) Φ_{PC} =1.7π, G=1300 (732KB); (b) Φ_{PC} =1.85π, G=1400 (442KB).

3. Conclusion

In conclusion, we have numerically studied the operation of a high peak power ultrashort pulse fiber laser. It is numerically shown that despite of the existence of local pulse breaking in the cavity as a result of strong nonlinear pulse compression process, due to the pulse circulation in a dispersion-managed cavity, the pulse breaking could be recovered by the laser cavity, and the laser can still emit stable ultrashort pulses. It is because of the strong nonlinear pulse compression, transform-limited pulse with bandwidth beyond the laser gain bandwidth could be generated in the laser.

Acknowledgment

This project is supported by the National Research Foundation Singapore under the contract NRF-G-CRP 2007-01.

#95964 - $15.00 USD Received 8 May 2008; revised 25 Jun 2008; accepted 13 Jul 2008; published 28 Jul 2008